28p

CODE 1

NASA TN D-1511

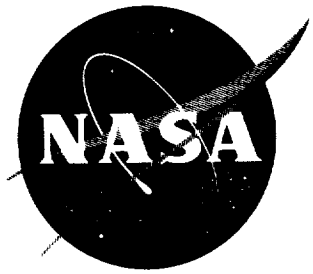

TECHNICAL NOTE

D-1511

LATERAL RANGE CONTROL BY BANKING DURING INITIAL PHASES OF SUPERCIRCULAR REENTRIES

By Donald L. Baradell

Langley Research Center
Langley Station, Hampton, Va.

NATIONAL AERONAUTICS AND SPACE ADMINISTRATION

WASHINGTON November 1962

NATIONAL AERONAUTICS AND SPACE ADMINISTRATION

TECHNICAL NOTE D-1511

LATERAL RANGE CONTROL BY BANKING DURING INITIAL PHASES OF SUPERCIRCULAR REENTRIES*

By Donald L. Baradell

SUMMARY

The feasibility of increasing the lateral range capability of reentry vehicles having low-lift-drag ratios, by allowing the vehicle to reenter in a banked attitude, is investigated. The effects of such banked reentries on allowable reentry corridor width and on lateral range capability are discussed. Numerical results are used throughout the investigation to furnish accurate evaluations of the effects being studied and to check the validity of some approximate relations presented. The heading-angle change developed during the initial pull-up by a vehicle reentering in a banked attitude is shown to produce significant increases in the lateral range achieved during reentry. Emphasis is placed on reentry at escape velocity but the results also apply in character to reentry at other supercircular velocities.

INTRODUCTION

The successful completion of any manned space mission implies the solution of two general problems - survival of the extreme heating and deceleration loads of reentry, and vehicle recovery. The survival problem implies the return of the vehicle to the earth's surface within vehicle and passenger tolerance limits. Most reentry research to date has focused on this problem. The recovery problem implies the ability to return the vehicle to some desired point on the earth's surface. For direct reentry from a near-lunar or a deep space mission, considerable variations in reentry point, reentry angle, and reentry plane must be anticipated. The reentry vehicle must, therefore, possess the ability to control its range after reentry in order to achieve the desired point return. Aerodynamic maneuvering can provide the desired control of range.

Recent studies have indicated that considerable ranges can be achieved by even low-lift-drag-ratio vehicles operating wholly within the atmosphere if proper maneuvering is accomplished early in the reentry while the vehicle is still

*The material presented herein is based on a thesis entitled "Range Control During Initial Phases of Supercircular Reentries" submitted in partial fulfillment of the requirements for the degree of Master of Science in Aerospace Engineering, Virginia Polytechnic Institute, Blacksburg, Virginia, May 1962.

traveling at supercircular speeds. Several modes of operation which are capable of providing range control at supercircular speeds are discussed in references 1 and 2. In reference 1, idealized maneuvers for achieving maximum and minimum ranges from given initial conditions are discussed, and approximate equations for these ranges are presented. In addition, reference 1 presents preliminary results obtained in a six-degree-of-freedom fixed-base analog simulator at the NASA Langley Research Center. These results indicate that a human pilot can perform satisfactorily the basic maneuvers required for range control at supercircular speeds.

These recent studies have considered initiating range control while the vehicle is traveling at supercircular speeds, but only after the initial pull-up has been performed, that is, after the initial flight-path angle has been reduced to zero. In considering longitudinal range, not much is lost in most cases by delaying range control until after the pull-up is completed since the range during pull-up comprises a small portion of the total achievable range. In considering lateral range control, however, small changes in heading angle during the initial pull-up can result in large lateral displacements of the landing point.

The present investigation explores the possibility of increasing the lateral range capability of reentry vehicles by allowing the vehicle to reenter the atmosphere in a banked attitude. The vehicle considered utilizes the "roll only" maneuver discussed in references 1 and 2. Equations are developed for the motion of a vehicle entering the atmosphere of a spherical nonrotating earth, and some permissible approximations to these equations are discussed. The effects of the banked reentry on the allowable supercircular reentry corridor and on the vehicle lateral range capability are determined. Numerical results obtained for the developed system of equations through use of an IBM 7090 electronic data processing system are used throughout the investigation to furnish accurate evaluations of the effects in question and to check the validity of the approximations used.

SYMBOLS

A	reference area
a_{ij}	metric tensor
C_D	drag coefficient (eq. (A19))
D	drag force
F_k	covariant tensor components of external force
$F_{(k)}$	physical components of external force
g	acceleration due to gravity

h	altitude above earth's surface
L	lift force
L_V	vertical component of lift force (eq. (1))
L_Y	lateral component of lift force (eq. (1))
m	mass of vehicle
R	resultant aerodynamic force
r	distance from center of earth (fig. 2)
T	kinetic energy (eq. (A2))
t	time
V	total velocity
V^k	contravariant tensor components of velocity
$V_{(k)}$	physical components of velocity
W	vehicle weight, mg
x^k	general coordinates ($k = 1, 2, 3$)
γ	flight-path angle (eq. (A11))
λ	lateral range angle (fig. 2)
$\Delta\lambda$	lateral-range-angle increment
ξ	heading angle (eq. (A11))
$\Delta\xi$	heading-angle change
ρ	density of atmosphere
φ	bank angle
ψ	longitudinal range angle (fig. 2)
ψ_c	longitudinal range angle available after completion of initial pull-up (fig. 9)

Subscripts:

e	evaluated at earth's surface

i,j,k	suffixes in range and summation convention (1, 2, 3)
o	initial reentry conditions
ov	overshoot conditions
un	undershoot conditions

Dots above quantities indicate differentiation with respect to time.

THEORETICAL MODEL CONSIDERED

This investigation considers the motion of a vehicle reentering the atmosphere of a spherical nonrotating earth under the influence of aerodynamic and gravitational forces. The simplified earth model was considered in this parametric study in order that results of a more general nature might be obtained. If the additional forces due to the rotation and oblateness of the earth are considered, separate solutions would be required for each reentry point and reentry direction. Any trajectory calculations of a final, specific nature should, of course, include these forces. For the simplified model used in this investigation, the reentry solutions are independent of the specific point and direction of reentry, and no generality is lost by assuming the reentry to occur in the equatorial plane.

The vehicle considered is an approximately flat-face type, which utilizes the "roll-only" mode of maneuvering discussed in references 1 and 2. A constant angle of attack, corresponding to vehicle maximum L/D, is maintained throughout the portion of the reentry considered. The resultant aerodynamic force is composed of a drag force opposite to the direction of motion, and a lift force normal to the drag, as shown in figure 1. By banking the vehicle, the lift force L is rotated about the drag force D giving rise to vertical and lateral components of lift, defined in terms of the bank angle φ.

$$\left.\begin{aligned} L_V &= L \cos \varphi \\ L_Y &= L \sin \varphi \end{aligned}\right\} \tag{1}$$

The view in figure 1(b) is along the flight path in the direction of the drag force. The resultant aerodynamic force R is in the plane of L and D, and the velocity vector is normal to the plane of the figure. The roll-only mode of operation is attractive from both the point of view of simplifying heat-protection requirements and from the standpoint of attitude control, as discussed in reference 1. The appropriate pitch for the desired L/D would be selected prior to reentry, and the vehicle would be trimmed in this attitude by either an offset center of gravity or a fixed-aerodynamic-flap type of pitch control (or a combination of the two). Variation of the vertical component of lift as necessary throughout the reentry can be accomplished by rolling the vehicle about the wind axis. If it is so desired, the lateral displacement introduced by such a maneuver

can be corrected for by alternating the direction of roll so as to affect a weaving motion about the desired flight path. For the type of vehicle considered, rolling moments are low and roll control could be accomplished economically by use of the same reaction-jet system used for roll stabilization in space. Use of reaction jets is generally not possible for pitch control because of the relatively large pitching moments involved.

REENTRY EQUATIONS

Coordinate System

The spherical coordinate system chosen for use in this investigation is indicated in figure 2. The position of the vehicle at any time is determined by the coordinates r, λ, and ψ. If the $\lambda = 0$ plane is taken as the equatorial plane, then λ corresponds to the geographical latitude and ψ is a measure of the geographic longitude on the earth's surface. Throughout this investigation, the reentry point is assumed given by $\lambda_o = 0$, $\psi_o = 0$, and $r_o = r_e + h_{atm}$ where r_e is the radius of the earth and h_{atm} is the height of the appreciable atmosphere, taken as 400,000 feet.

The derivation of the point-mass reentry equations, as used in this paper, is presented in the appendix. The resulting set of equations (eqs. (A17) to (A25)) includes the effects of the earth sphericity on the reentry path as discussed in reference 1.

Method of Numerical Solution

The set of equations considered is readily amenable to numerical solution by a finite difference procedure. For the numerical results presented in this paper, these equations were programed for an IBM 7090 electronic data processing system. The solutions were obtained by considering an incremental increase of time, the length of which was allowed to vary in order to assure sufficient linearity of all dependent variables over the time increment considered. For these numerical calculations the 1959 ARDC model atmosphere (ref. 3) was used. All numerical results presented in this paper are for a vehicle reentering the atmosphere at escape velocity, taken as 36,500 ft/sec, and for a vehicle with W/C_DA of 50 lb/sq ft, which is considered appropriate for manned vehicles in the L/D range considered.

Reentry Corridor

The reentry corridor, as used in this paper, is defined by the following limits: The undershoot limit is taken as the steepest angle at which the vehicle can enter at a constant, positive value of L_V/D without exceeding a deceleration of 10g. The overshoot limit is taken as the shallowest angle at which the vehicle can enter at a constant, negative value of L_V/D so that at the bottom

of pull-up ($\gamma = 0$) the vehicle can hold a constant altitude by rolling to full negative L_V/D (i.e., $\varphi = 180^\circ$). The constant-altitude requirement for the overshoot limit is based on the results of simulator studies, reference 1, which indicate that for shallow reentry angles control becomes difficult if even a small positive flight-path angle is allowed to develop after pull-up.

The available reentry-angle spread, as determined from machine results, for unbanked low L/D vehicles reentering the atmosphere at escape speed is shown in figure 3. For these reentries, the undershoot limit corresponds to reentry at $L_V/D = L/D$, and the overshoot limit, to reentry at $L_V/D = -L/D$.

As can be seen from figure 3, the corridor width is a strong function of L/D, especially for the low values considered. Most of the effect of L/D, in increasing corridor width, is achieved by values of L/D less than unity. The present investigation is limited to values of L/D in this range, with particular concentration on vehicles with $L/D = 0.5$.

EFFECTS OF BANKED REENTRY ON REENTRY CORRIDOR

Effect on Undershoot Limit

Since corridor width is strongly dependent on vehicle L_V/D, it is directly affected by the use of bank during reentry. A vehicle of given L/D, entering in a banked attitude, will follow the same altitude-velocity curve as a lower L/D unbanked vehicle with the same value of L_V/D. The resultant aerodynamic force R acting on a vehicle is, however, dependent on the vehicle total L/D. This force is given by

$$\frac{R}{W} = \frac{1}{2}\rho V^2 \frac{C_D A}{W}\sqrt{1 + \left(\frac{L}{D}\right)^2} \qquad (2)$$

The dynamic pressure $\frac{1}{2}\rho V^2$ is dependent only on the altitude-velocity curve for vehicles of equal $\frac{W}{C_D A}$. The banked vehicle considered will, therefore, experience greater resultant loads, because of its higher L/D, than the lower L/D unbanked vehicle of equal L_V/D. Conversely, the reentry angle for a 10g deceleration limit will be shallower for the banked vehicle. The extent to which banking affects the undershoot limit for a parabolic reentry is indicated in figure 4. The reentry angle which will produce a maximum deceleration of 10g is plotted against the L_V/D employed.

Reentries over a range of reentry angles were considered for vehicles with L/D between 0 and 1 and values of φ from 0° to 90°. In figure 4 the solid line, obtained from figure 3, shows the limiting undershoot angles for unbanked vehicles. The dashed lines show the limits, as determined from machine results,

for vehicles with $L/D = 0.5$ and 1, which reenter at various bank angles φ, thus varying the value of L_V/D. As can be seen, the limiting angles for a banked vehicle with $L/D = 0.5$ are only slightly less than those for an unbanked vehicle entering at the same L_V/D. For the banked reentry at $L/D = 1$, the differences are considerably larger.

Effect on Overshoot Limit

If operation near the overshoot limit is considered, negative lift is required in order to overcome the tendency of the vehicle to skip out of the atmosphere. At any given altitude and velocity, a vehicle operating at full negative L_V/D obviously employs more force in the earthward direction than a vehicle of the same L/D operating at a lesser bank angle.

On the other hand, consider the reentry of two vehicles operating at different values of L/D but at the same negative value of L_V/D. This could be the case if the higher L/D vehicle reenters at some bank angle between 90° and 180°, and the lower L/D vehicle reenters at $\varphi = 180^\circ$. The descent paths of the two vehicles during the initial pull-up would be identical. At the bottom of the pull-up, however, the higher L/D vehicle would have the capability of rolling to $\varphi = 180^\circ$ in order to exert more force earthward than the lower L/D vehicle which is already at full negative L_V/D. Thus, the higher L/D vehicle could maintain constant altitude after pull-up for shallower reentries than the lower L/D vehicle performing the same pull-up. In other words, a higher L/D banked vehicle can successfully reenter at shallower angles than a lower L/D unbanked vehicle reentering at the same value of L_V/D. This result is illustrated in figure 5, which shows the variation of corridor overshoot limit with vehicle L_V/D. The solid line, obtained from figure 3, applies to a vehicle employing full negative L_V/D. The dashed lines apply to vehicles with $L/D = 0.5$ and 1, which reenter at values of φ between 90° and 180°, thus achieving different values of L_V/D.

The comparison of banked and unbanked vehicles on the basis of the same value of L_V/D is not to be interpreted as a valid measure of the effect of bank on corridor width. Obviously, the true measure of this effect for a vehicle of given L/D capability is a comparison of corridor width for a vehicle utilizing bank with the corridor width for the same vehicle utilizing either full positive or full negative lift only. The purpose of presenting the results in the form of a comparison on the basis of L_V/D is to show how the reduction in corridor width due to bank compares with the reduction that would be expected due to the lower effective lift force.

The allowable span of reentry angles for banked and unbanked ($\cos \varphi = \pm 1$) vehicles, obtained from figures 4 and 5, is presented in figure 6. Although the banked vehicle with $L/D = 1$ shows considerably smaller allowable spans than the unbanked vehicle, the banked vehicle with $L/D = 0.5$ shows allowable spans

which compare favorably with the spans for the unbanked vehicle. In addition, the banked vehicle generates a lateral force which can be useful in extending lateral range capability.

EFFECT OF BANKED PULL-UP ON LATERAL RANGE

Lateral Force and Heading-Angle Change During Pull-Up

In considering the development of lateral range and change in heading angle during the initial pull-up, it is to be noted from the foregoing discussion that the amount of lift available for lateral force depends on the position of the vehicle path in the reentry corridor. Near the extremes of this corridor, it is necessary to direct a certain amount of lift in the vertical direction to either alleviate the deceleration load or to avoid skipping. Some limitations are, therefore, placed on the bank angle that can be used near these extremes. The extent of these limitations for a vehicle with $L/D = 0.5$ reentering at escape speed, as determined from machine results, is shown in figure 7. Near the overshoot limit, bank angles below the skip boundary, extending from $\gamma_o = -4.71$ to $\gamma_o = -5.02$, would allow insufficient lift in the earthward direction to prevent skipping. Near the undershoot limit, bank angles above the indicated deceleration boundary, extending from $\gamma_o = -5.87$ to $\gamma_o = -7.5$, would allow insufficient lift in the positive vertical direction and excessive deceleration would result. In the reentry angle range from -5.02° to -5.87° the pull-up could be accomplished at maximum bank ($\varphi = 90^\circ$) without surpassing either corridor limit.

The amount of lateral force which is available to the vehicle considered in figure 7 for the range of allowable reentry angles is presented in figure 8. Near-maximum values of L_Y/D are seen to be available throughout much of the corridor.

The lateral force used produces a lateral displacement and a heading-angle change. The lateral displacement which is obtained during the initial phases of reentry is small compared to the total lateral range which can be obtained. The heading-angle change, however, can contribute significantly to the total lateral range as indicated in figure 9.

In this sketch, four reentry-path traces are shown corresponding to different bank, no-bank combinations. The quantity ψ_c is the longitudinal range angle available to the vehicle after pull-up, $\Delta\xi$ is the heading-angle change obtained during pull-up, and $\Delta\lambda$ is the lateral-range-angle increment due to the use of bank during pull-up.

The trace OA corresponds to the path the vehicle would follow if no lateral displacement were desired; OC is the path for a vehicle banking after the initial pull-up only; OB corresponds to a vehicle banking during the initial pull-up but not after; OD is the trace of a vehicle using bank throughout the reentry. The trace OB indicates the manner in which bank during the initial pull-up can affect lateral range. Although the heading-angle change during pull-up is small, considerable lateral range is obtained because of the characteristically large

values of ψ_c. If the lateral displacement during pull-up is neglected, this lateral-range increment is given by spherical trigonometry as

$$\tan(\Delta\lambda) = \tan(\Delta\xi)\sin\psi_c \tag{3}$$

Approximate Equation for Heading-Angle Change

Throughout the initial phases of reentry, γ is small so that $\cos\gamma \approx 1$ and $\sin\gamma \approx 0$. With these assumptions, equations (A20), (A22), and (A24) become

$$\frac{dV}{dt} = -\frac{D}{m} \tag{4}$$

$$\frac{d\xi}{dt} = \frac{L\sin\varphi}{mV} - \frac{V}{r}\cos\xi\tan\lambda \tag{5}$$

$$\frac{d\psi}{dt} = \frac{V\cos\xi}{r\cos\lambda} \tag{6}$$

Combining equations (5) and (6) and using equation (1) leads to

$$d\xi = \frac{L_Y}{mV}dt - \sin\lambda\, d\psi \tag{7}$$

The first term in equation (7) is the heading change due to aerodynamic forces, and the second term is due to the sphericity of the earth model considered. For the moderate ranges and small lateral displacements achieved during the initial pull-up, this sphericity term may be neglected. If equation (7) is then combined with equation (4) there results

$$d\xi = -\frac{L_Y}{D}\frac{dV}{V} \tag{8}$$

which is readily integrated for constant L_Y/D to give

$$\xi = -\frac{L_Y}{D}\log_e\frac{V}{V_o} \tag{9}$$

where integration is started at $V = V_o$ and $\xi = \xi_o = 0$. As a check on the validity of the approximations used, values obtained from equation (9) are compared with exact numerical values of ξ in figure 10. The numerical computations were for a vehicle with $L/D = 0.5$ reentering at $V_o = 36{,}500$ ft/sec. The vehicle was banked prior to reentry and maintained a constant bank angle throughout the pull-up. The data points presented are conditions at the bottom of the pull-up for reentries throughout the allowable reentry corridor. The higher values of V for any given bank angle correspond to the shallower reentries.

For the cases for which $\varphi = 90^\circ$, the last data point presented corresponds to the reentry in which satellite velocity is achieved at the bottom of pull-up. Beyond this value no pull-up point is defined as the flight-path angle will remain negative throughout the reentry. Good agreement between numerical results and values predicted by equation (9) exists for all cases considered.

The amount of heading-angle change achieved during pull-up can also be obtained from figure 10. Values of ξ on the order of 0.05 radian are seen to be attainable throughout much of the corridor.

It should be noted that, in obtaining equation (9), the flight-path angle γ was taken to be approximately zero and effects of the earth's sphericity were neglected. Equation (9) is, therefore, the same equation as would be obtained for the heading-angle change in planar, level flight. Although these approximations are valid for the initial phases of reentry, caution should be exercised in applying them to other portions of the trajectory where larger flight-path angles or ranges may be involved.

Evaluations of Lateral Range Increment

The lateral range increment due to banked reentry is directly dependent on the longitudinal range the vehicle attains after pull-up (eq. (3)), and is thus dependent on the particular ranging maneuver employed after pull-up. For a given ranging maneuver after pull-up and a corresponding heading-angle change prior to the start of that maneuver, the lateral-range-angle increment due to banked reentry can be evaluated. In figure 11, values of this increment, as given by equation (3), are presented for the ranges of the variables $\Delta\xi$ and ψ_c of interest.

In reference 1, lateral and longitudinal ranges for vehicles performing two reentry maneuvers are presented as a function of the velocity at which the maneuver is initiated. These maneuvers are begun shortly after pull-up. In figure 10 of this paper, values of heading-angle change developed by a vehicle in decelerating from reentry velocity to a given velocity are shown. Although the data points in figure 10 correspond to conditions at the bottom of pull-up, the curves presented are valid for some distance beyond this point, as long as the assumptions of small flight-path angle, small lateral displacement, and moderate range apply.

These heading-angle changes can be coupled with the ranges presented in figure 6 of reference 1, and this pair of values can be used in figure 11 of this paper to evaluate the lateral-range-angle increment.

As an example, consider a vehicle of $L/D = 0.5$ reentering at a 40° bank angle and maintaining this attitude until $V = 31{,}000$ ft/sec. From figure 10, the heading-angle change developed to this point is about 0.052 radian. From figure 6 of reference 1 the range available from this point is found to be about 1.5 earth radii if the maximum range mode of operation is used. From figure 11, for $\psi_c = 1.5$ and $\Delta\xi = 0.052$, a value of $\Delta\lambda$ of about 0.05 radian is obtained.

This is the lateral-range-angle increment due to the banked pull-up considered. In figure 16 of reference 1, the lateral range available without a banked pull-up for this reentry is seen to be about 0.12 earth radian, so that the banked pull-up can provide about a 40-percent increase in lateral range for this case.

CONCLUDING REMARKS

The feasibility of reentering the atmosphere from a supercircular orbit with a low-lift-drag-ratio L/D vehicle in a banked attitude has been studied. Emphasis was placed on reentry at escape velocity, but the effects determined for this case should also apply in character to reentry at other supercircular speeds.

The corridor limits for reentry at escape velocity were found to be affected by the banked pull-up in the manner expected. The limiting undershoot and overshoot angles for a banked vehicle were both found to be shallower than the corresponding limits for an unbanked vehicle with the same ratio of vertical lift to drag L_V/D and ballistic parameter W/C_DA.

The variation of allowable reentry-angle span with L_V/D for a banked vehicle with $L/D = 0.5$ was found to follow closely the variation with L_V/D appropriate to equivalent unbanked vehicles.

The amount of lateral force which can be used near the corridor extremes is limited by vertical-lift requirements, but near-maximum lateral force can be used throughout most of the corridor for a vehicle with $L/D = 0.5$.

The heading-angle change developed during the initial pull-up by a vehicle reentering in a banked attitude can produce significant increases in the total lateral range achieved during the reentry.

Langley Research Center,
National Aeronautics and Space Administration,
Langley Station, Hampton, Va., August 24, 1962.

APPENDIX

DERIVATION OF EQUATIONS OF MOTION

The Lagrangian equations for the motion of a particle under the influence of external forces can be written in index notation (ref. 4) as

$$\frac{d}{dt}\left(\frac{\partial T}{\partial \dot{x}^k}\right) - \frac{\partial T}{\partial x^k} = F_k \tag{A1}$$

The quantity T is the kinetic energy of the particle. The suffix k takes on the values 1, 2, and 3 for the three-dimensional space considered. In general coordinates the kinetic energy is given by

$$T = \frac{m}{2} a_{ij} \dot{x}^i \dot{x}^j \tag{A2}$$

where suffixes repeated an even number of times indicate summation and the dot indicates differentiation with respect to time. The derivatives of T are therefore

$$\frac{\partial T}{\partial \dot{x}^k} = m a_{ik} \dot{x}^i \tag{A3}$$

$$\frac{\partial T}{\partial x^k} = \frac{m}{2} \dot{x}^i \dot{x}^j \frac{\partial a_{ij}}{\partial x^k} \tag{A4}$$

and the equations of motion can be written as

$$m \frac{d}{dt}\left(a_{ik} \dot{x}^i\right) - \frac{m}{2} \dot{x}^i \dot{x}^j \frac{\partial a_{ij}}{\partial x^k} = F_k \tag{A5}$$

For the coordinate system used in this paper (see fig. 2), the metric tensor is

$$a_{ij} = \begin{bmatrix} 1 & 0 & 0 \\ 0 & (x^1)^2 & 0 \\ 0 & 0 & (x^1 \cos x^2)^2 \end{bmatrix} \tag{A6}$$

where $x^1 = r$, $x^2 = \lambda$, $x^3 = \psi$. The covariant tensor components of the external forces acting on the vehicle F_k are related to the physical force components $F_{(k)}$ by the expression

$$F_k = \sqrt{a_{kk}} F_{(k)} \tag{A7}$$

The contravariant tensor components of the velocity V^k are given by

$$V^k = \dot{x}^k \tag{A8}$$

and are related to the physical velocity components $V_{(k)}$ through the expression

$$V_{(k)} = \sqrt{a_{kk}} V^k = \sqrt{a_{kk}} \dot{x}^k \tag{A9}$$

and the total velocity is given by

$$V = \sqrt{V_{(k)} V_{(k)}} = \sqrt{(\dot{r})^2 + (r\dot{\lambda})^2 + (r \cos \lambda \, \dot{\psi})^2} \tag{A10}$$

If the flight-path angle γ and the heading angle ξ defined by

$$\left.\begin{aligned} \gamma &= \sin^{-1} \frac{V_{(r)}}{V} = \sin^{-1} \frac{\dot{r}}{V} \\ \xi &= \tan^{-1} \frac{V_{(\lambda)}}{V_{(\psi)}} = \tan^{-1}\left(\frac{r\dot{\lambda}}{r \cos \lambda \, \dot{\psi}}\right) \end{aligned}\right\} \tag{A11}$$

are introduced, then from equations (A10) and (A11)

$$\left.\begin{aligned} \dot{r} &= V \sin \gamma \\ \dot{\psi} &= \frac{V \cos \gamma \cos \xi}{r \cos \lambda} \\ \dot{\lambda} &= \frac{V \cos \gamma \sin \psi}{r} \end{aligned}\right\} \tag{A12}$$

Differentiating equations (A12) yields

$$\left.\begin{aligned} \ddot{r} &= \dot{V} \sin \gamma + \dot{\gamma} V \cos \gamma \\ \ddot{\psi} &= \frac{1}{r \cos \lambda}\left[\dot{V} \cos \gamma \cos \xi - \dot{\xi} V \cos \gamma \sin \xi - \dot{\gamma} V \sin \gamma \cos \xi \right. \\ &\quad \left. + \frac{(V \cos \gamma)^2}{r}(\sin \xi \cos \xi \tan \lambda - \tan \gamma \cos \xi)\right] \\ \ddot{\lambda} &= \frac{1}{r}\left(\dot{V} \cos \gamma \sin \xi + \dot{\xi} V \cos \gamma \cos \xi - \dot{\gamma} V \sin \gamma \sin \xi - \frac{V^2}{r} \sin \gamma \cos \gamma \sin \xi\right) \end{aligned}\right\} \tag{A13}$$

The physical components of the external forces are given by

$$\left.\begin{aligned} F_{(r)} &= L \cos \varphi \cos \gamma - D \sin \gamma - mg \\ F_{(\lambda)} &= -L \cos \varphi \sin \gamma \sin \xi + L \sin \varphi \cos \xi - D \cos \gamma \sin \xi \\ F_{(\psi)} &= -L \cos \varphi \sin \gamma \cos \xi - L \sin \varphi \sin \xi - D \cos \gamma \cos \xi \end{aligned}\right\} \tag{A14}$$

where L and D are the aerodynamic lift and drag forces, respectively, and φ is the vehicle bank angle. (See fig. 1.)

Substituting equations (A6) and (A7) into equation (A5) gives

$$\left.\begin{aligned} \ddot{r} - r(\dot{\lambda})^2 - r \cos^2\lambda(\dot{\psi})^2 &= \frac{F_{(r)}}{m} \\ r\ddot{\lambda} + 2\dot{\lambda}\dot{r} + r \sin \lambda \cos \lambda(\dot{\psi})^2 &= \frac{F_{(\lambda)}}{m} \\ r \cos \lambda \ddot{\psi} + 2 \cos \lambda \dot{\psi}\dot{r} - 2r \sin \lambda \dot{\psi}\dot{\lambda} &= \frac{F_{(\psi)}}{m} \end{aligned}\right\} \tag{A15}$$

If equations (A12), (A13), and (A14) are then substituted into equation (A15), three equations in $\dot{V}$, $\dot{\gamma}$, and $\dot{\xi}$ are obtained which can be solved to yield

$$\left.\begin{aligned} \dot{V} &= -\frac{D}{m} - g \sin \gamma \\ \dot{\gamma} &= \frac{L \cos \varphi}{mV} - \frac{g \cos \gamma}{V} + \frac{V \cos \gamma}{r} \\ \dot{\xi} &= \frac{L \sin \varphi}{mV \cos \gamma} - \frac{V \cos \gamma \tan \lambda \cos \xi}{r} \end{aligned}\right\} \tag{A16}$$

Equations (A12) and (A16) provide six equations in six dependent variables (r, ψ, λ, V, γ, and ξ). The quantities L/D, W/C_DA, and φ are considered given. The variables ρ and g can be related to r through the relations

$$g = g_e\left(\frac{r_e}{r}\right)^2 \tag{A17}$$

$$\rho = \rho(h) = \rho(r - r_e) \tag{A18}$$

where r_e is the radius of the earth and g_e is the acceleration of gravity at the earth's surface. An appropriate density-altitude relation is chosen for equation (A18).

If the drag coefficient defined by

$$C_D \equiv \frac{D}{\frac{1}{2}\rho V^2 A} \tag{A19}$$

and the vehicle weight W are introduced, the complete system of equations of motion can be written as

$$\frac{1}{g}\frac{dV}{dt} = -\frac{1}{2}\rho V^2 \frac{C_D A}{W} - \sin\gamma \tag{A20}$$

$$\frac{1}{g}\frac{d\gamma}{dt} = \frac{1}{2}\rho V \frac{C_D A}{W}\frac{L}{D}\cos\varphi - \frac{\cos\gamma}{V}\left(1 - \frac{V^2}{gr}\right) \tag{A21}$$

$$\frac{1}{g}\frac{d\xi}{dt} = \frac{1}{2}\rho V \frac{C_D A}{W}\frac{L}{D}\frac{\sin\varphi}{\cos\gamma} - \frac{V}{gr}\cos\gamma\cos\xi\tan\lambda \tag{A22}$$

$$\frac{dr}{dt} = V\sin\gamma \tag{A23}$$

$$\frac{d\psi}{dt} = \frac{V\cos\gamma\cos\xi}{r\cos\lambda} \tag{A24}$$

$$\frac{d\lambda}{dt} = \frac{V\cos\gamma\sin\xi}{r} \tag{A25}$$

REFERENCES

1. Becker, J. V., Baradell, D. L., and Pritchard, E. B.: Aerodynamics of Trajectory Control for Re-Entry at Escape Speed. Astronautica Acta, Vol. VII, Fasc. 5-6, 1961, pp. 334-358.

2. Mandell, Donald S.: Maneuvering Performance of Lifting Re-Entry Vehicles. ARS Jour., vol. 32, no. 3, Mar. 1962, pp. 346-354.

3. Minzner, R. A., Champion, K. S. W., and Pond, H. L.: The ARDC Model Atmosphere, 1959. Air Force Surveys in Geophysics No. 115 (AFCRC-TR-59-267), Air Force Cambridge Res. Center, Aug. 1959.

4. Synge, J. L., and Schild, A.: Tensor Calculus. Univ. of Toronto Press, 1949.

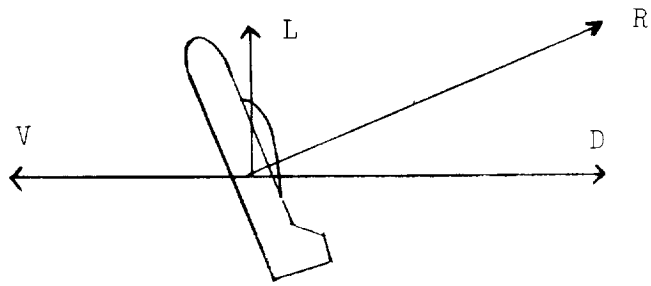

(a) Side view, $\varphi = 0$.

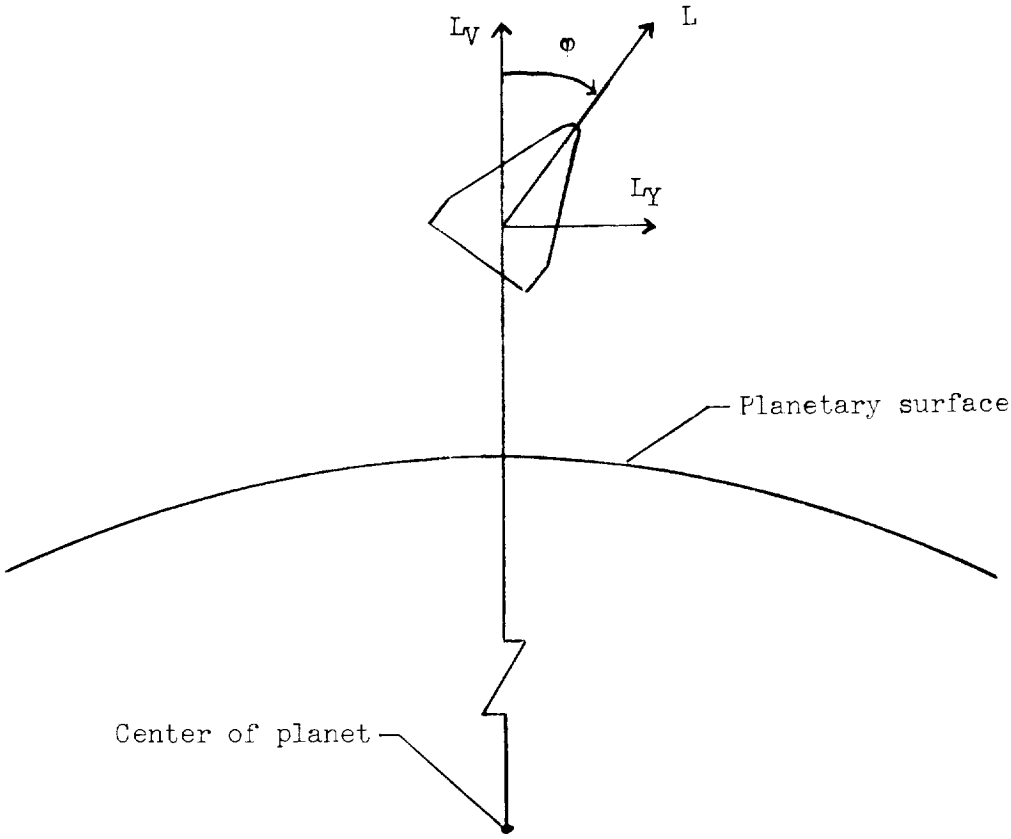

(b) Front view, $\gamma = 0$.

Figure 1.- Sketch of aerodynamic forces acting on reentry vehicle.

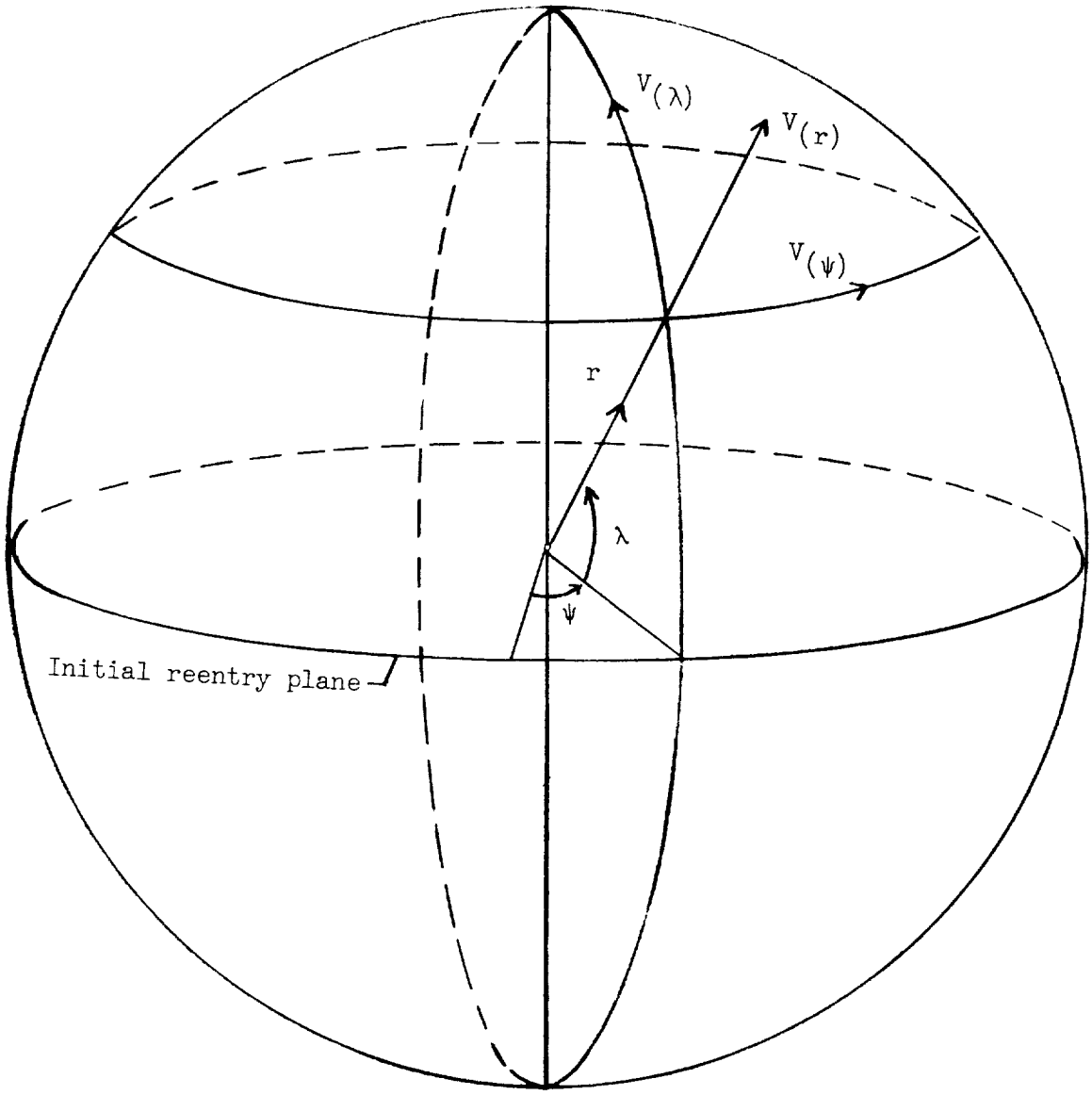

Figure 2.- Coordinate system for reentry equations.

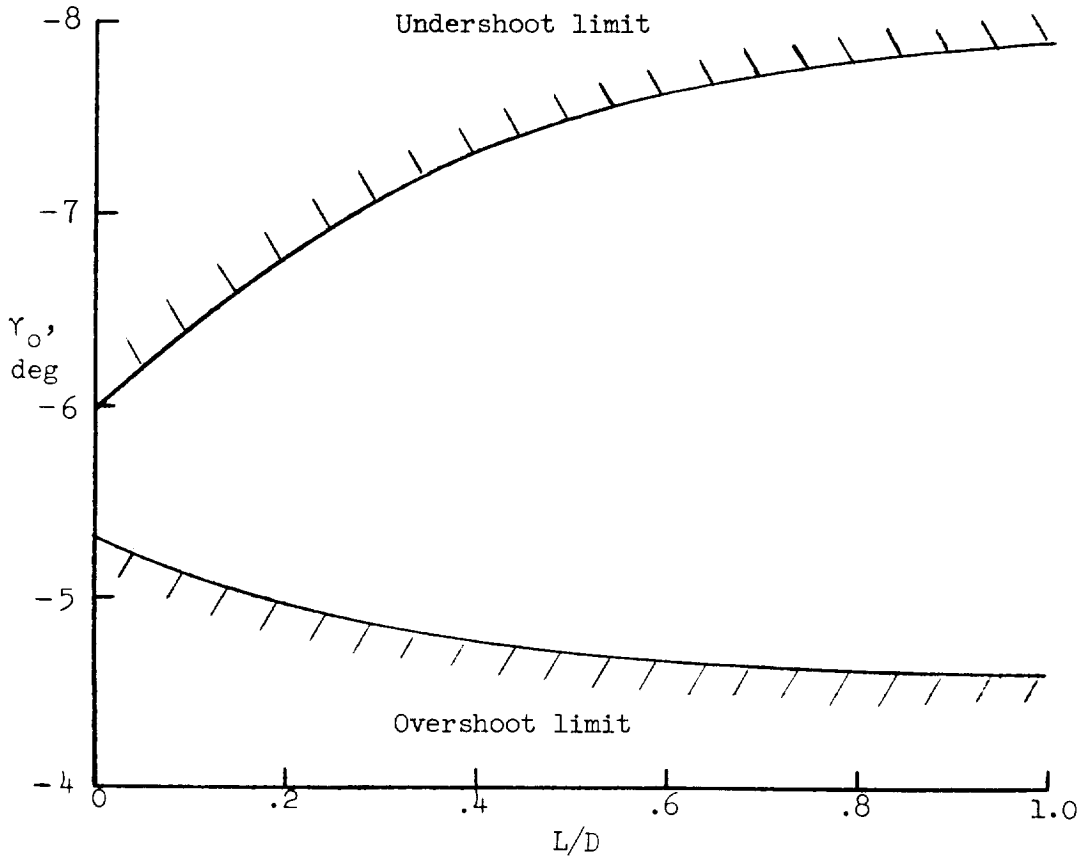

Figure 3.- Reentry-angle limits. V_o = 36,500 ft/sec; W/C_DA = 50 lb/sq ft.

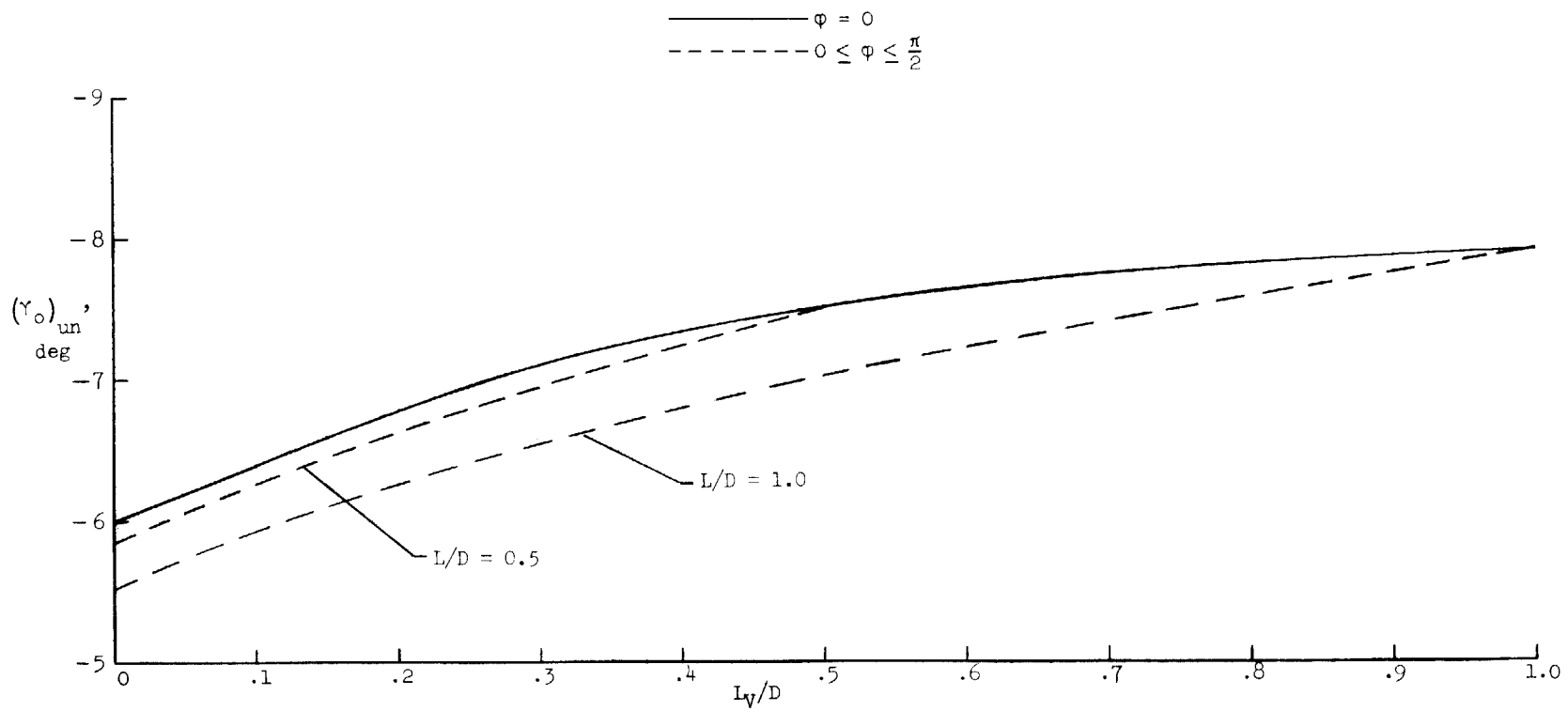

Figure 4.- Effect of banked reentry on undershoot limit. V_o = 36,500 ft/sec; W/C_DA = 50 lb/sq ft.

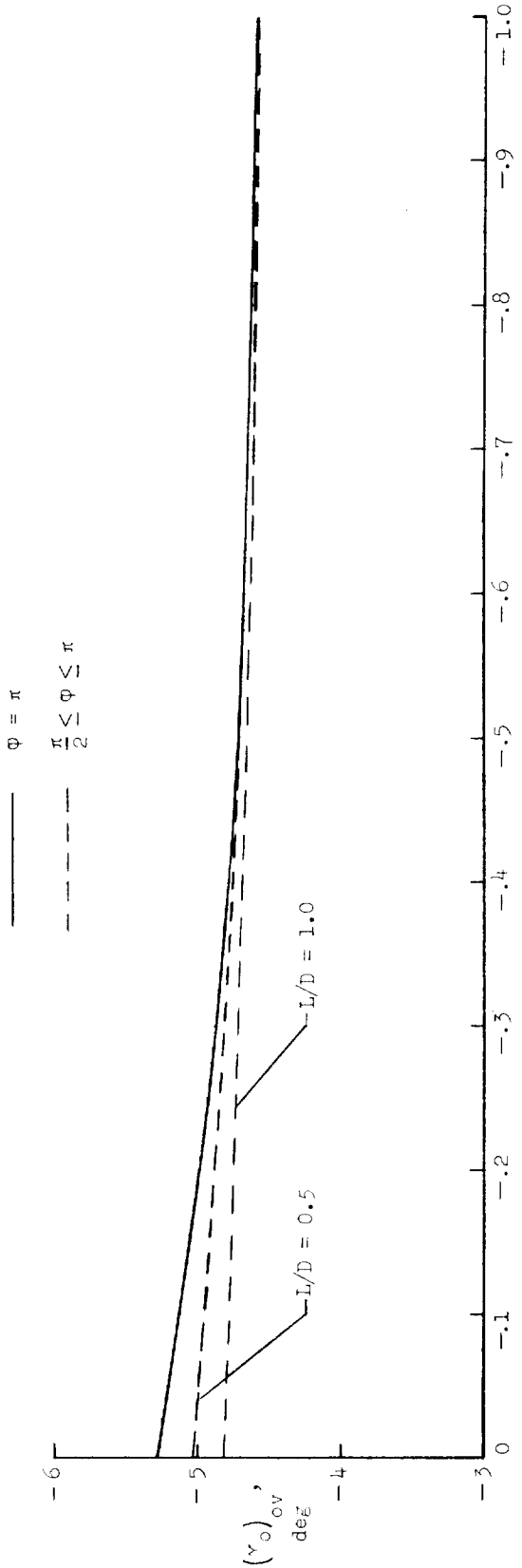

Figure 5.- Effect of banked reentry on overshoot limit. V_o = 36,500 ft/sec; W/C_DA = 50 lb/sq ft.

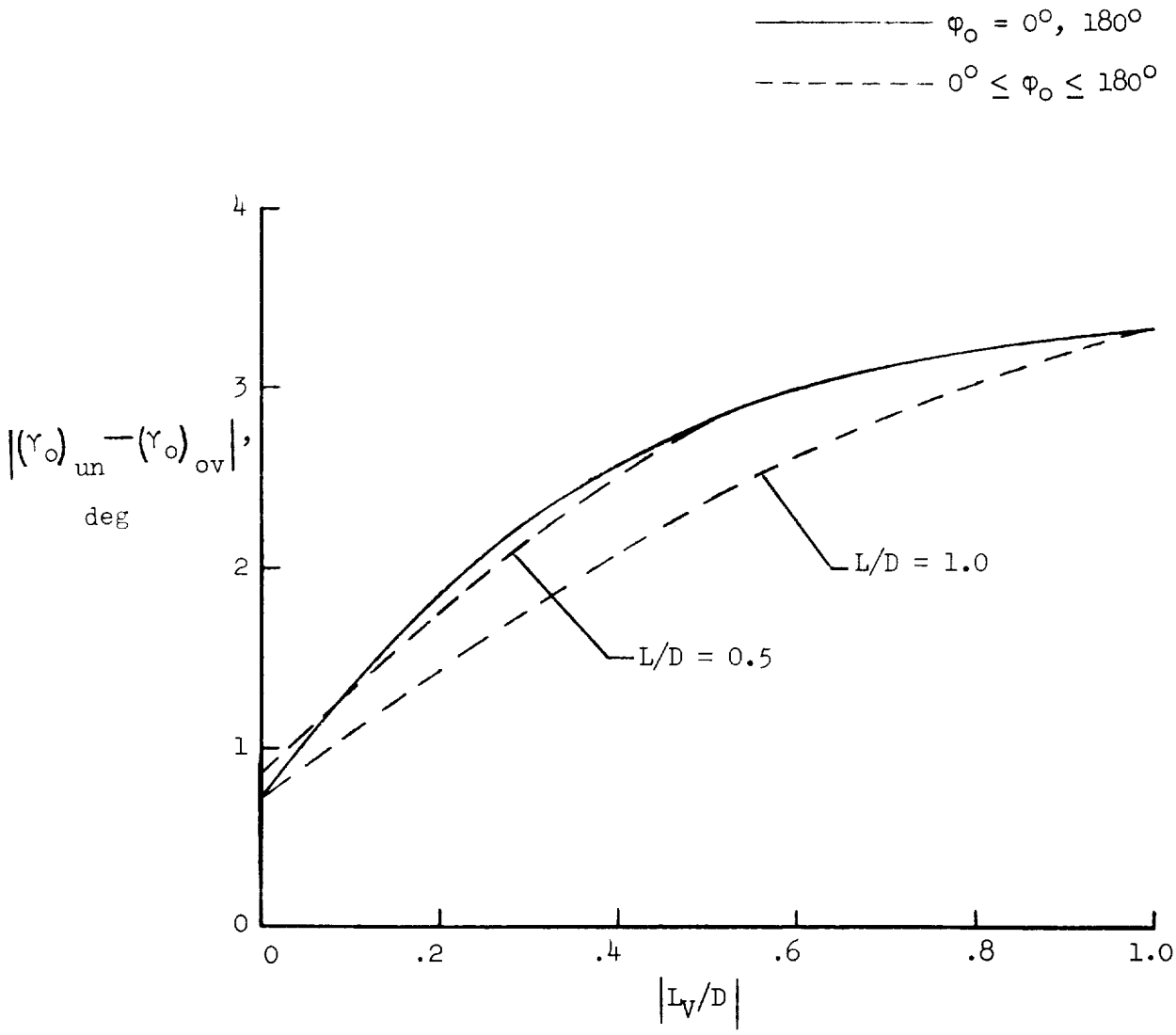

Figure 6.- Allowable span of reentry angles within defined corridor. V_o = 36,500 ft/sec; W/C_DA = 50 lb/sq ft.

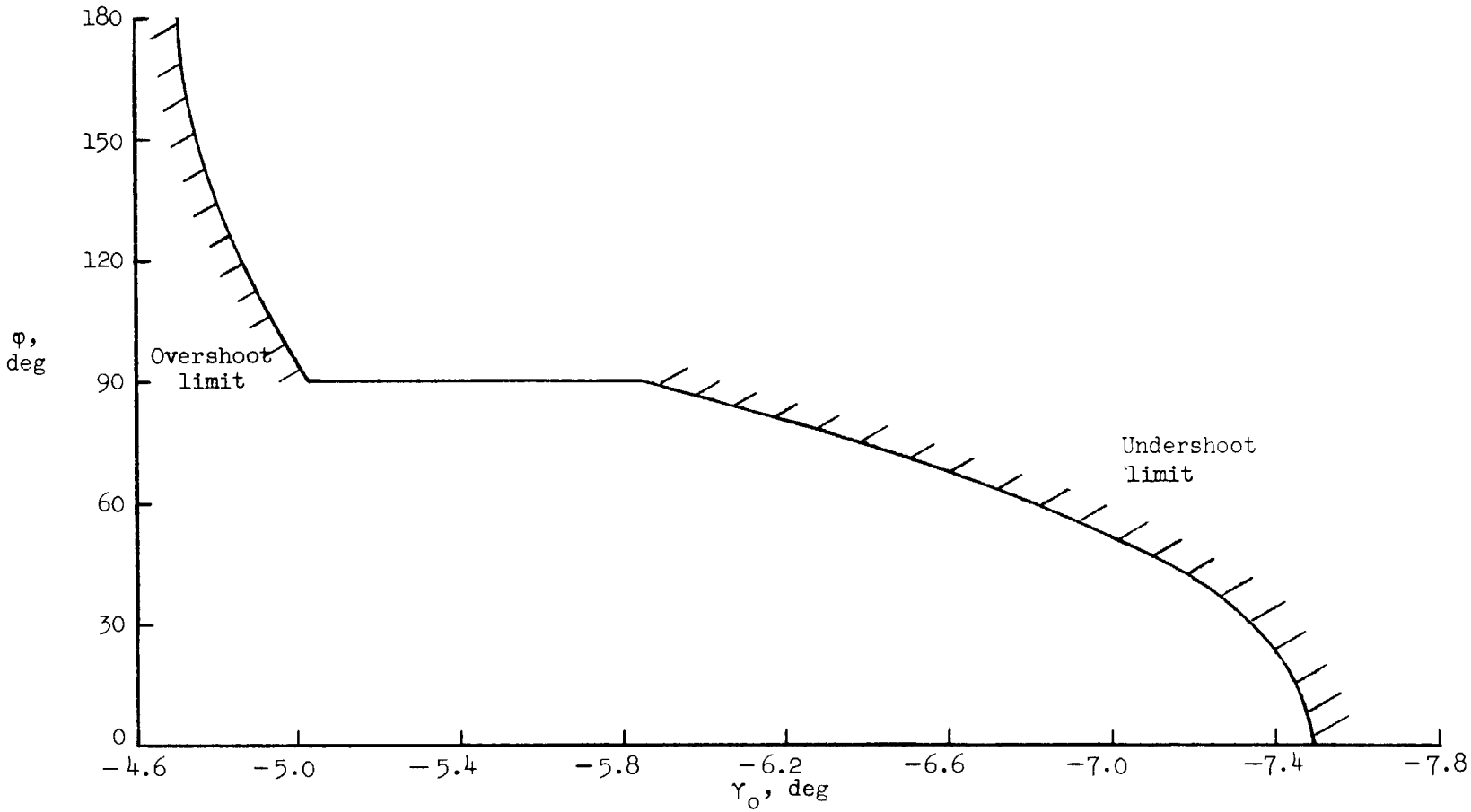

Figure 7.- Bank-angle limits during pull-up. L/D = 0.5; V_o = 36,500 ft/sec; W/C_DA = 50 lb/sq ft.

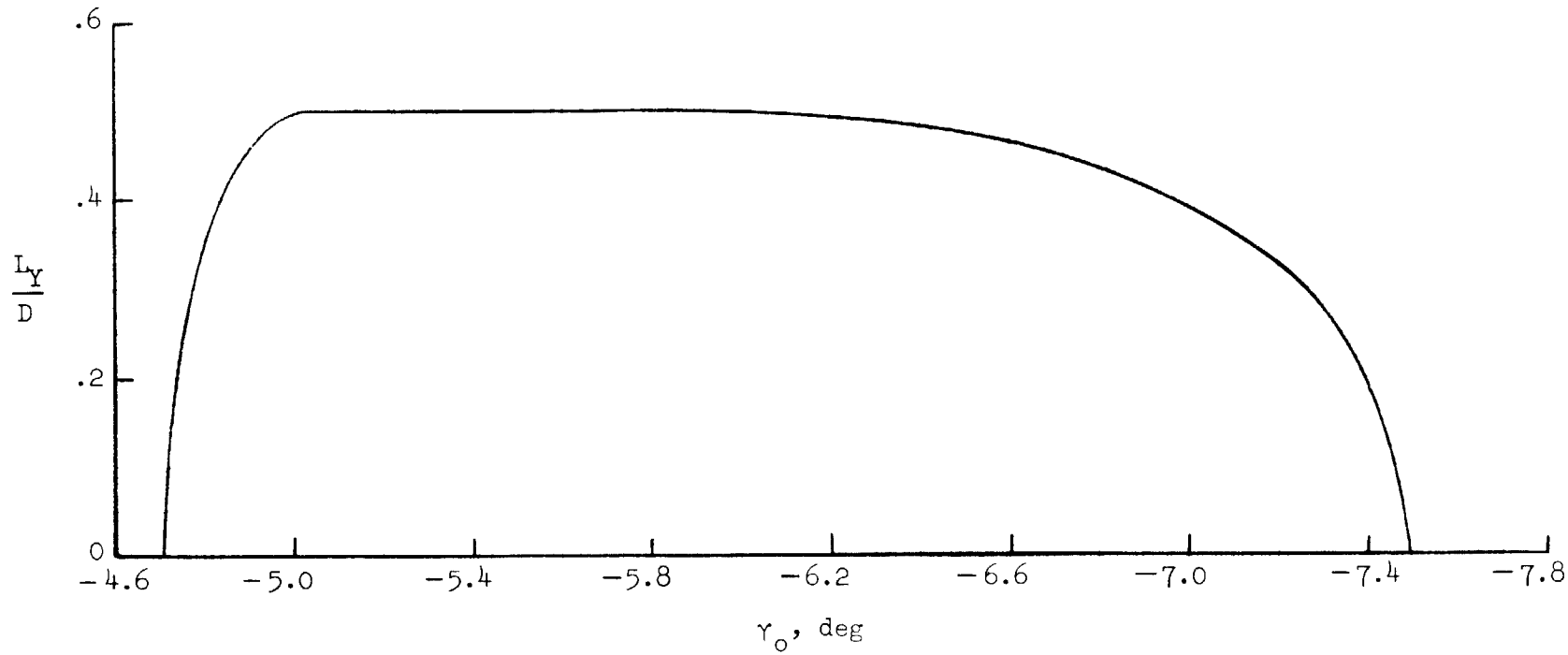

Figure 8.- Available side force during pull-up. L/D = 0.5; V_o = 36,500 ft/sec; W/C_DA = 50 lb/sq ft.

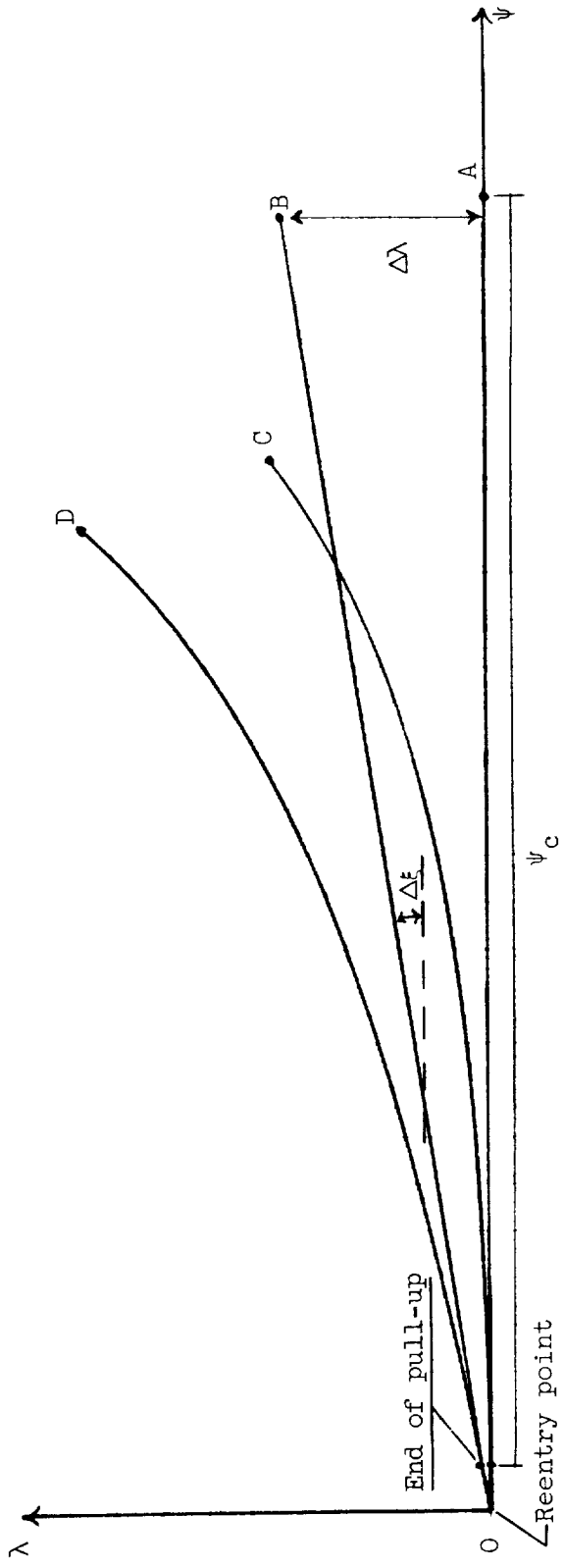

Figure 9.- Use of bank during pull-up to increase lateral range.

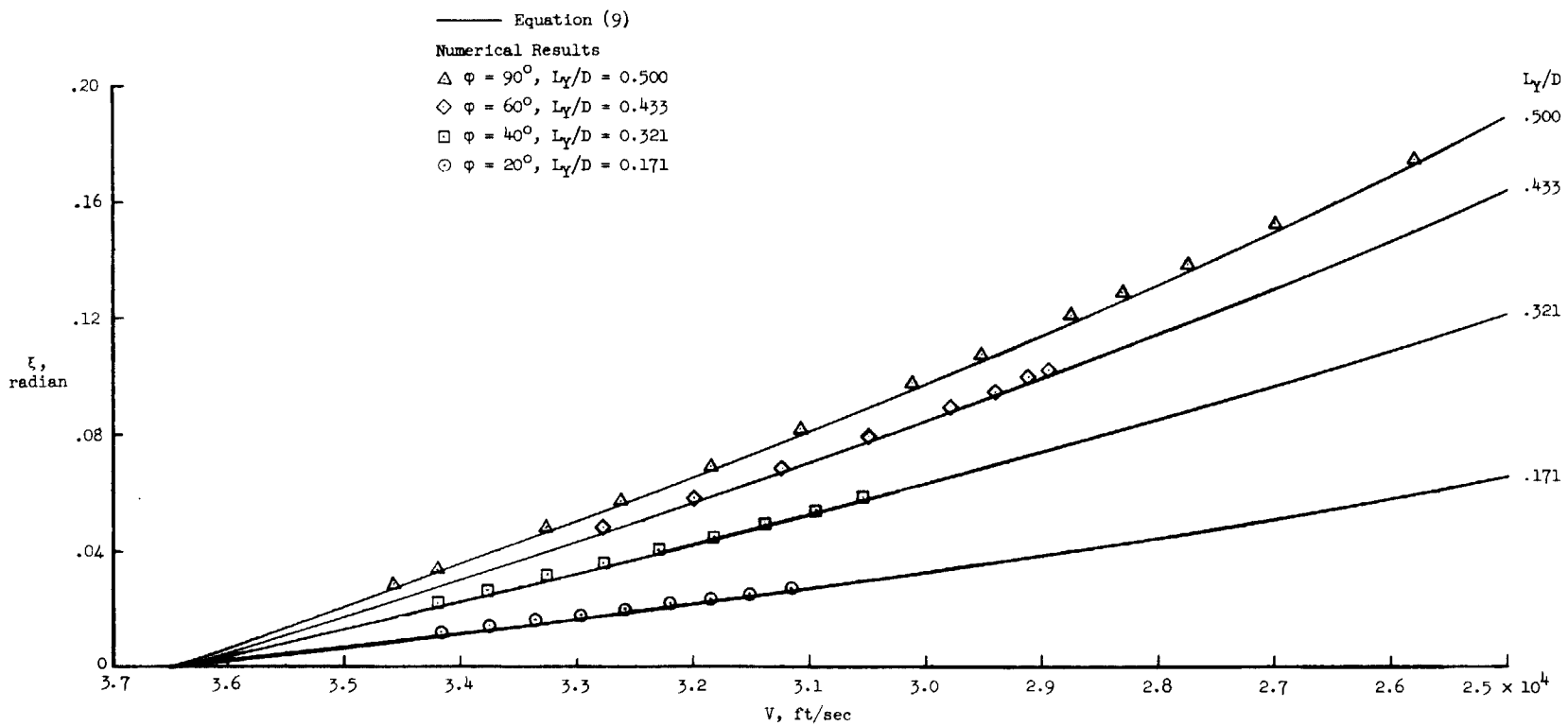

Figure 10.- Heading-angle change during initial phases of reentry. L/D = 0.5; V_o = 36,500 ft/sec; W/C_DA = 50 lb/sq ft.

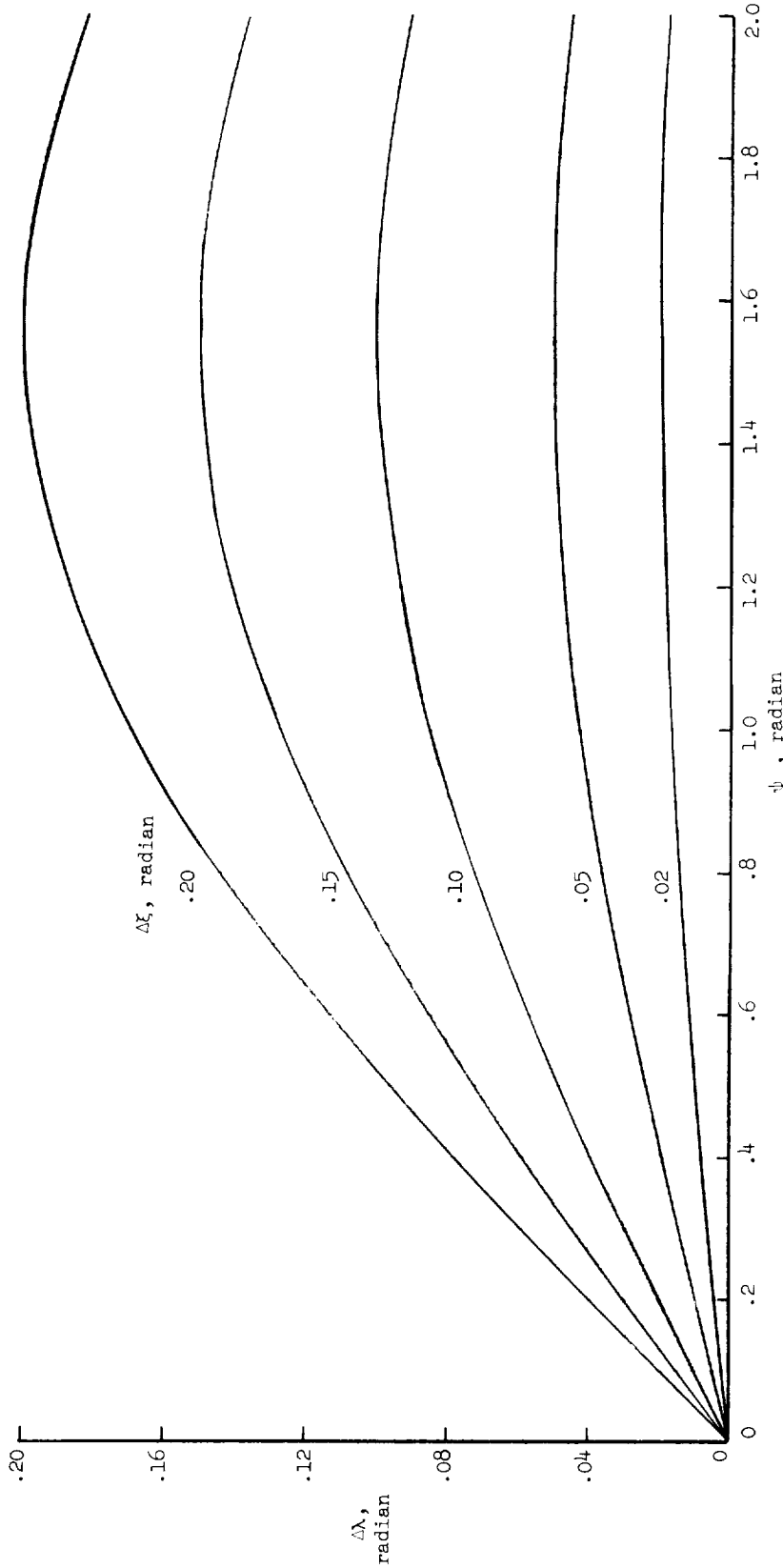

Figure 11.- Lateral-range-angle increment due to banked pull-up. tan $(\Delta\lambda)$ = tan $(\Delta\xi)$ sin ψ_c.

NASA TN D-1511
National Aeronautics and Space Administration.
LATERAL RANGE CONTROL BY BANKING DURING INITIAL PHASES OF SUPERCIRCULAR REENTRIES. Donald L. Baradell. November 1962. 27p. OTS price, $0.75. (NASA TECHNICAL NOTE D-1511)

The feasibility of increasing the lateral range capability of reentry vehicles having low-lift-drag ratios, by allowing the vehicle to reenter in a banked attitude, is investigated. The effects of such banked reentries on allowable reentry corridor width and on lateral range capability are discussed. Numerical results are used throughout the investigation to furnish accurate evaluations of the effects being studied and to check the validity of some approximate relations presented. The heading-angle change developed during the initial pull-up by a vehicle reentering in a banked attitude is shown to produce significant increases in the lateral range achieved during reentry. Emphasis is placed on reentry at escape velocity but the results also apply in character to reentry at other supercircular velocities.

I. Baradell, Donald L.
II. NASA TN D-1511

NASA

NASA TN D-1511
National Aeronautics and Space Administration.
LATERAL RANGE CONTROL BY BANKING DURING INITIAL PHASES OF SUPERCIRCULAR REENTRIES. Donald L. Baradell. November 1962. 27p. OTS price, $0.75. (NASA TECHNICAL NOTE D-1511)

The feasibility of increasing the lateral range capability of reentry vehicles having low-lift-drag ratios, by allowing the vehicle to reenter in a banked attitude, is investigated. The effects of such banked reentries on allowable reentry corridor width and on lateral range capability are discussed. Numerical results are used throughout the investigation to furnish accurate evaluations of the effects being studied and to check the validity of some approximate relations presented. The heading-angle change developed during the initial pull-up by a vehicle reentering in a banked attitude is shown to produce significant increases in the lateral range achieved during reentry. Emphasis is placed on reentry at escape velocity but the results also apply in character to reentry at other supercircular velocities.

I. Baradell, Donald L.
II. NASA TN D-1511

NASA

NASA TN D-1511
National Aeronautics and Space Administration.
LATERAL RANGE CONTROL BY BANKING DURING INITIAL PHASES OF SUPERCIRCULAR REENTRIES. Donald L. Baradell. November 1962. 27p. OTS price, $0.75. (NASA TECHNICAL NOTE D-1511)

The feasibility of increasing the lateral range capability of reentry vehicles having low-lift-drag ratios, by allowing the vehicle to reenter in a banked attitude, is investigated. The effects of such banked reentries on allowable reentry corridor width and on lateral range capability are discussed. Numerical results are used throughout the investigation to furnish accurate evaluations of the effects being studied and to check the validity of some approximate relations presented. The heading-angle change developed during the initial pull-up by a vehicle reentering in a banked attitude is shown to produce significant increases in the lateral range achieved during reentry. Emphasis is placed on reentry at escape velocity but the results also apply in character to reentry at other supercircular velocities.

I. Baradell, Donald L.
II. NASA TN D-1511

NASA

NASA TN D-1511
National Aeronautics and Space Administration.
LATERAL RANGE CONTROL BY BANKING DURING INITIAL PHASES OF SUPERCIRCULAR REENTRIES. Donald L. Baradell. November 1962. 27p. OTS price, $0.75. (NASA TECHNICAL NOTE D-1511)

The feasibility of increasing the lateral range capability of reentry vehicles having low-lift-drag ratios, by allowing the vehicle to reenter in a banked attitude, is investigated. The effects of such banked reentries on allowable reentry corridor width and on lateral range capability are discussed. Numerical results are used throughout the investigation to furnish accurate evaluations of the effects being studied and to check the validity of some approximate relations presented. The heading-angle change developed during the initial pull-up by a vehicle reentering in a banked attitude is shown to produce significant increases in the lateral range achieved during reentry. Emphasis is placed on reentry at escape velocity but the results also apply in character to reentry at other supercircular velocities.

I. Baradell, Donald L.
II. NASA TN D-1511

NASA